Letter

Anomalous transient blueshift in the internal stretch mode of CO/Pd(111)

Raúl Bombín,[1,2,3,*] A. S. Muzas,[2] Dino Novko,[4] J. Iñaki Juaristi,[1,2,5,†] and Maite Alducin[2,5,‡]

[1]*Departamento de Polímeros y Materiales Avanzados: Física, Química y Tecnología, Facultad de Químicas (UPV/EHU), Apartado 1072, E-20080 Donostia-San Sebastián, Spain*

[2]*Centro de Física de Materiales CFM/MPC (CSIC-UPV/EHU), Paseo Manuel de Lardizabal 5, E-20018 Donostia-San Sebastián, Spain*

[3]*Departament de Física, Universitat Politècnica de Catalunya, Campus Nord B4-B5, E-08034 Barcelona, Spain*

[4]*Institute of Physics, Bijenička 46, HR-10000 Zagreb, Croatia*

[5]*Donostia International Physics Center (DIPC), Paseo Manuel de Lardizabal 4, E-20018 Donostia-San Sebastián, Spain*

(Received 15 November 2022; revised 13 February 2023; accepted 1 March 2023; published 10 March 2023)

In time-resolved pump-probe vibrational spectroscopy the internal stretch mode of polar molecules is utilized as a key observable to characterize the ultrafast dynamics of adsorbates on surfaces. The adsorbate nonadiabatic intermode couplings are the commonly accepted mechanisms behind the observed transient frequency shifts. Here, we study the CO/Pd(111) system with a robust theoretical framework that includes electron-hole pair excitations and electron-mediated coupling between the vibrational modes. A mechanism is revealed that screens the electron-phonon interaction and originates a blueshift under ultrafast nonequilibrium conditions. The results are explained in terms of the abrupt change in the density of states around the Fermi level, and are instrumental for understanding the dynamics at multicomponent surfaces involving localized and standard *s* or *p* states.

DOI: 10.1103/PhysRevB.107.L121404

The use of intense femtosecond laser pulses opened a new and efficient pathway to initiate reactions at surfaces. The interplay between laser-induced hot electrons and the nuclear degrees of freedom offers the possibility of activating the adsorbates dynamics within the subpicosecond timescale. As such, femtosecond laser pulses have extensively been used to trigger diverse elementary processes such as adsorbate desorption [1,2], diffusion [3], and different chemical reactions [4,5]. The main challenge is to understand how the highly excited electrons couple to the adsorbate dynamics and how this energy flows into the different vibrational modes.

Femtosecond pump-probe vibrational spectroscopy permits tracking in the time domain the adsorbate dynamics initiated by the pump laser pulse with unprecedented time resolution [6]. The internal stretch (IS) vibrational mode of dipolar adsorbates, having a very distinct frequency, appears as the good observable to be followed over the reaction coordinate [7,8]. Several experiments have been made on Ru, Ir, Pt, and Cu surfaces including different coverages of CO and NO molecules [8–15]. In all those cases, the IS mode frequency exhibits a fast redshift, followed by a slower recovery in the timescale of picoseconds. The frequency shifts are explained within the widely established models in terms of couplings to the low-energy CO modes and possible changes in the adsorption site. In both cases, it is the increasing and decreasing population of the CO antibonding $2\pi^*$ that is thought to cause the weakening and strengthening of the IS mode, respectively. An important assumption in these models is that the IS mode only brings information on the adsorbate dynamics. However, there are examples showing that there might be other factors contributing to the transient frequency changes. This is the case of the blueshift observed in the rather more complex system formed by CO molecules coordinated to ruthenium tetraphenylporphyrin on a Cu(110) surface [16], which neither the intermode couplings nor the adsorption site changes are able to explain.

In this Letter we study the ultrafast transient dynamics of 0.5 ML of CO on the Pd(111) surface, using the theoretical framework of Ref. [17] that correctly reproduced the experimental ultrafast time-resolved vibrational spectra of CO on Cu(100) [15]. Our calculations predict an unusual blueshift occurring within the subpicosecond timescale that is not related to the commonly accepted intermode coupling, but to the peculiar properties of the surface electronic structure. In solids, the electron-phonon scattering strength is expected to increase with the electronic temperature causing a softening in the frequency because more electrons participate in the interaction [18,19]. This is what explained the subpicosecond redshift in the CO/Cu(100) system [17]. Here, we show that the strong reduction of the Pd(111) density of states around the Fermi level can revert this normal behavior at extreme laser-induced high temperatures. Hence the predicted blueshift of the IS mode brings information on the surface electronic structure rather than the intermode couplings. The present results show that dipolar molecules can serve alternatively as a direct probe of the ultrafast electron dynamics of metal surfaces, providing time-dependent chemical potential shifts, the structure of density of states, electron temperatures, and coupling strengths.

*raul.bombin@ehu.eus
†josebainaki.juaristi@ehu.eus
‡maite.alducin@ehu.eus

The transient vibrational spectra of the CO adlayer is calculated, following Ref. [17], in terms of the phonon self-energy expressed up to second order in the electron-phonon (*e*-ph) interaction, i.e., $\pi_\lambda(\omega, \mathbf{q}) \approx \pi_\lambda^{[1]}(\omega, \mathbf{q}) + \pi_\lambda^{[2]}(\omega, \mathbf{q})$, where λ, ω, and $\mathbf{q}$ denote the index, energy, and momentum of the phonon mode, respectively. In the femtosecond pump-probe experiments of interest, the CO molecules are initially prepared with their IS mode vibrating in phase by illuminating them with an IR pulse. Thus, only the $\mathbf{q} = 0$ excitations are considered.

The expression for the first-order term that exclusively accounts for the electron-hole pair (de)excitations [i.e., the usual nonadiabatic coupling (NC)] reads [20]

$$\pi_\lambda^{[1]}[\omega; T_e(t)] = \sum_{\mu\mu'\mathbf{k}\sigma} \left|g_\lambda^{\mu\mu'}(\mathbf{k}, 0)\right|^2 \frac{f(\epsilon_{\mu\mathbf{k}}) - f(\epsilon_{\mu'\mathbf{k}})}{\omega + \epsilon_{\mu\mathbf{k}} - \epsilon_{\mu'\mathbf{k}} + i\eta}, \quad (1)$$

where μ, $\mathbf{k}$, and $\epsilon_{\mu\mathbf{k}}$ are the electron band index, momentum, and energy, respectively; $g_\lambda^{\mu\mu'}(\mathbf{k}, \mathbf{q})$ are the *e*-ph matrix elements; and the summation over σ accounts for the spin degrees of freedom. The function $f(\epsilon_{\mu\mathbf{k}}) = 1/(e^{\beta[\epsilon_{\mu\mathbf{k}} - \mu(T_e)]} + 1)$ is the Fermi-Dirac distribution function, where $\beta = 1/(k_B T_e)$, k_B is the Boltzmann constant, T_e is the electronic temperature, and $\mu(T_e)$ is the chemical potential at T_e. Following previous works [20,21], we fix the broadening parameter to a finite, physically motivated value of 30 meV [22,23]. As it will soon become apparent, in the above expression not only the *e*-ph matrix elements, but also the Pd(111) electronic structure are crucial to understand the ultrafast transient dynamics of the CO adlayer.

Equation (1) only contains interband contributions [20], and the first nonvanishing intraband processes that can affect the CO vibrational dynamics are those involved in the coupling of the IS mode with other phonons. In the framework of many-body perturbation theory, these electron-mediated phonon-phonon coupling (EMPPC) processes are included in the second-order intraband phonon self-energy term that reads [21,24],

$$\pi_\lambda^{[2]}[\omega; T_e(t), T_l(t)] = -\sum_{\mu\mu'\mathbf{k}\sigma,\lambda'\mathbf{k}'} \left|g_\lambda^{\mu\mu}(\mathbf{k}, 0)\right|^2 \left[1 - \frac{g_\lambda^{\mu'\mu'}(\mathbf{k}', 0)}{g_\lambda^{\mu\mu}(\mathbf{k}, 0)}\right] \left|g_{\lambda'}^{\mu\mu'}(\mathbf{k}, \mathbf{q}')\right|^2 \times \sum_{s,s'=\pm 1} \frac{f(\epsilon_{\mu\mathbf{k}}) - f(\epsilon_{\mu'\mathbf{k}'} - s's\omega_{\mathbf{q}'\lambda'})}{\epsilon_{\mu\mathbf{k}} - (\epsilon_{\mu'\mathbf{k}'} - s's\omega_{\mathbf{q}'\lambda'})} \frac{s[n_b(s\omega_{\mathbf{q}'\lambda'}) + f(s'\epsilon_{\mu'\mathbf{k}'})]}{\omega[\omega + i\eta + s'(\epsilon_{\mu\mathbf{k}} - \epsilon_{\mu'\mathbf{k}'}) + s\omega_{\mathbf{q}'\lambda'}]}, \quad (2)$$

where $\mathbf{q}' = \mathbf{k}' - \mathbf{k}$ and $n_b(\omega_{\mathbf{q},\lambda}) = 1/(e^{\beta\omega_{\mathbf{q}\lambda}} - 1)$ is the Bose-Einstein distribution, with $\beta = 1/(k_B T_l)$ and T_l the lattice temperature. The contribution of the vertex correction [second term in the square brackets of Eq. (2)], which is expected to be small [25], is neglected to reduce the computational cost. Finally, we use the two-temperature model (TTM) [26] to describe the excitation induced by the femtosecond pump pulse in the system as two coupled (nonequilibrated) heat thermal baths. It provides us with the temporal evolution of T_e and T_l that are used to evaluate Eqs. (1) and (2). The transient frequency shift due to *e*-ph coupling is obtained from the real part of the phonon self-energy as $\Delta\omega(t) \approx \mathrm{Re}[\pi_\lambda(\omega, t)] - \mathrm{Re}[\pi_\lambda(\omega, 0)]$. Obviously, the contributions to $\Delta\omega(t)$ from the first- and second-order terms will be $\Delta\omega^{[1]}(t) \approx \mathrm{Re}[\pi_\lambda^{[1]}(\omega, t)] - \mathrm{Re}[\pi_\lambda^{[1]}(\omega, 0)]$ and $\Delta\omega^{[2]}(t) \approx \mathrm{Re}[\pi_\lambda^{[2]}(\omega, t)] - \mathrm{Re}[\pi_\lambda^{[2]}(\omega, 0)]$, respectively.

At 0.5 ML, CO adsorbs on Pd(111) with an overall $c(4 \times 2)$ symmetry that consists of two coexisting structures, in which the CO molecules either occupy bridge sites [$c(4 \times 2)$-$2CO_{br}$] or the fcc and hcp hollow sites [$c(4 \times 2)$-$2CO_{hw}$] [27]. The results obtained in both structures for the experimental conditions under consideration are qualitatively similar. Thus, only the results for the $c(4 \times 2)$-$2CO_{br}$ structure are discussed here. The inset in Fig. 1(a) shows a top view of the supercell used in these calculations, which includes four Pd layers with two CO molecules in the adlayer, and 12.9 Å of vacuum.

All the calculations are based on density functional theory and the Bayesian error estimation functional with van der Waals correlation (BEEF-vdW) [28], as implemented in the QUANTUM ESPRESSO package [29,30]. In particular, the electron-phonon Wannier (EPW) code [31,32] is used to evaluate the *e*-ph coupling matrix elements. All the computational details and parameters that are needed to reproduce the results presented here are described in the Supplemental Material [33].

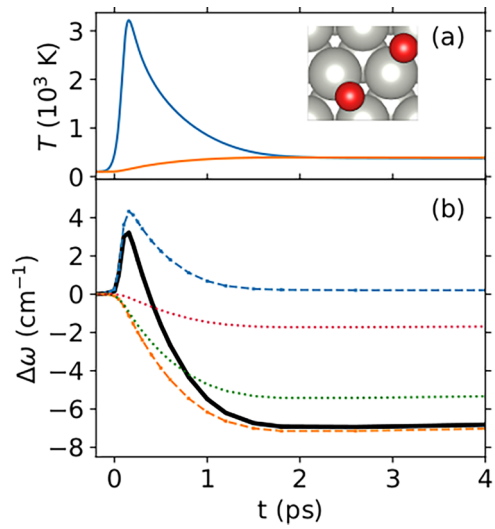

FIG. 1. Transient changes induced in CO/Pd(111) by a 450 nm pump pulse (100 fs duration and absorbed fluence of 40 J/m^2) that hits the surface at $t = 0.1$ ps. The initial temperature is 100 K. (a) Electron $T_e(t)$ (blue) and lattice $T_l(t)$ (orange) temperatures calculated with TTM. Inset: Top view of the $c(4 \times 2)$-$2CO_{br}$ unit cell. (b) Transient frequency shift of the CO IS mode: $\Delta\omega(t)$ (black solid), $\Delta\omega^{[1]}(t)$ (blue dashed), and $\Delta\omega^{[2]}(t)$ (orange dashed). Contributions of the CO and surface phonons to $\Delta\omega^{[2]}(t)$ are shown by red- and green-dotted lines, respectively.

Figure 1(b) contains the central result of this Letter. The black curve shows that upon exciting the surface with a 450 nm pump laser pulse, the CO IS mode exhibits an unexpected fast initial blueshift that contrasts to the usual redshift that has been observed in other metal surfaces by all previous time-resolved pump-probe vibrational spectroscopy experiments [9–15]. The predicted blueshift occurs within the first hundreds of femtoseconds, reaches a maximum value of $\approx 3\ \mathrm{cm}^{-1}$, and progressively vanishes giving rise to a late steady redshift of about $-7\ \mathrm{cm}^{-1}$. The comparison between the time evolution of the transient frequency shift $\Delta\omega(t)$ and that of the electronic and phononic temperatures, $T_e(t)$ and $T_l(t)$ [Fig. 1(a)], suggests that the initial blueshift and subsequent redshift follow $T_e(t)$ and $T_l(t)$, respectively.

By analyzing the contribution to $\Delta\omega(t)$ coming from the first-order interband NC term $\Delta\omega^{[1]}(t)$ and the second-order intraband EMPPC term $\Delta\omega^{[2]}(t)$ [blue- and orange-dashed lines in Fig. 1(b), respectively], it is evident that the blueshift is caused by the coupling to the laser-induced hot electrons. This (positive) NC contribution, which is fully ruled by the time evolution of T_e, dominates the IS transient frequency during the initial instants in which $T_e \gg T_l$. The subsequent redshift is caused by the coupling to other system phonons via electron-hole pairs. This (negative) EMPPC contribution, which clearly increases following $T_l(t)$, dominates the frequency changes as T_l increases above 300 K, being responsible of the almost steady redshift observed at $t \geqslant 1$ ps. Interestingly, a slow steady redshift of comparable magnitude was observed for similar pump laser fluences in CO/Pt(111) [13], for which the transient lattice temperatures are expected to be equally large. Figure 1(b) also shows that the EMPPC contribution is dominated by the coupling to the Pd(111) phonons (green-dotted lines) rather than to the rest of CO modes (red-dotted lines). Note that both the surface and the CO adlayer phonons contribute to the EMPPC redshift, discarding any similarity between the present blueshift induced by hot electrons and the blueshift observed under thermal conditions on Ni(111) [34] and Pd(100) [35], explained in terms of anharmonic coupling between the CO vibrational modes.

The above analysis reveals a different mechanism behind the subpicosecond transient blueshift that is correlated to the T_e dependence of the nonadiabatic coupling between the IS mode and the laser-induced hot electrons. One naively should expect an enhancement in the e-ph scattering strength as temperature rises. This is what would cause the transient subpicosecond redshift in the CO/Cu(100) system found by both experiments [15] and theory [17]. Thus, the obtained NC blueshift suggesting an effective screening of the e-ph interaction by the hot electrons is somehow anomalous. It must be related to the peculiarities of the CO/Pd(111) electronic structure. Compared to the mentioned CO/Cu(100) system, the presence of the d-band edge near ε_F causes a sharp decrease of the CO/Pd(111) density of states (DOS) around the Fermi level [see Fig. 2(a)]. As T_e increases, the population and depopulation of states above and below $\mu(T_e)$ compensate each other, assuring conservation of the number of electrons N_e. Thus, the CO/Pd(111) chemical potential shifts to higher energies to counterbalance the strong asymmetry of the DOS around ε_F. Figure 2(b) shows that the

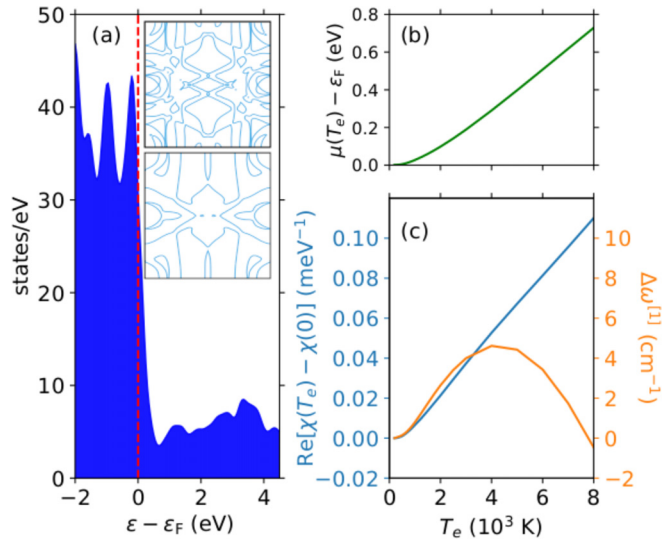

FIG. 2. (a) Electronic DOS of the CO/Pd(111) system. Vertical red dashed line marks the Fermi level. Insets: Constant energy cuts of the band structure over the Brillouin zone at $\epsilon = \mu(T_e)$ for $T_e = 100$ K (top) and $T_e = 3000$ K (bottom). (b) Dependence of the chemical potential with the electronic temperature. (c) Change in the real part of χ (blue) and in $\Delta\omega^{[1]}$ (orange) as a function of T_e.

chemical potential, which is calculated numerically by solving iteratively the equality, $N_e = \int \mathrm{DOS}(\epsilon) f[\epsilon, T_e, \mu(T_e)] d\epsilon$, increases by 0.2 eV when T_e raises from 100 to 3000 K. Such an increase is enough to induce an important reduction in the DOS around $\mu(T_e)$, i.e., the states that are likely to contribute to the e-ph interaction. To illustrate it, the constant energy cuts of the CO/Pd(111) band structure with the plane $\epsilon = \mu(T_e)$ are shown across the whole Brillouin zone in the insets of Fig. 2(a) for $T_e = 100$ K (top) and $T_e = 3000$ K (bottom). There is an evident reduction of the electronic states that would support the above interpretation of the blueshift as a weakening of the e-ph interaction. The results calculated with $\mu(T_e) = \varepsilon_F$ further confirm this idea [33].

The dependence of the NC term $\Delta\omega^{[1]}$ on T_e is not monotonic. As shown in Fig. 2, $\Delta\omega^{[1]}(T_e)$ (orange curve, right axis) initially increases with T_e up to reaching its maximum value at around 4000 K and it starts to decrease, becoming negative at temperatures larger than 7000 K. There are two factors ruling the first-order phonon self-energy $\pi^{[1]}$ that can affect the temperature dependence of $\Delta\omega^{[1]}$, the e-ph matrix elements, and the electronic structure. To disentangle each contribution, it is useful to evaluate the response function $\chi(\omega)$ under the constant matrix element approximation [36], that reads

$$\chi(\omega) = \sum_{\mu\mu'\mathbf{k}\sigma} \frac{f(\epsilon_{\mu\mathbf{k}}) - f(\epsilon_{\mu'\mathbf{k}})}{\omega + \epsilon_{\mu\mathbf{k}} - \epsilon_{\mu'\mathbf{k}} + i\eta}. \tag{3}$$

Mathematically, the above expression coincides with setting the e-ph matrix elements to one in the first-order phonon self-energy expression [cf. Eq. (1)], allowing us to single out the effect of the electronic structure in the temperature dependence of $\pi^{[1]}(\omega, T_e)$. Figure 2(c) shows that the change in the real part of the response function (blue, left axis) grows monotonically with T_e in contrast to the nonmonotonous behavior of $\Delta\omega^{[1]}$. Altogether, these results suggest that the

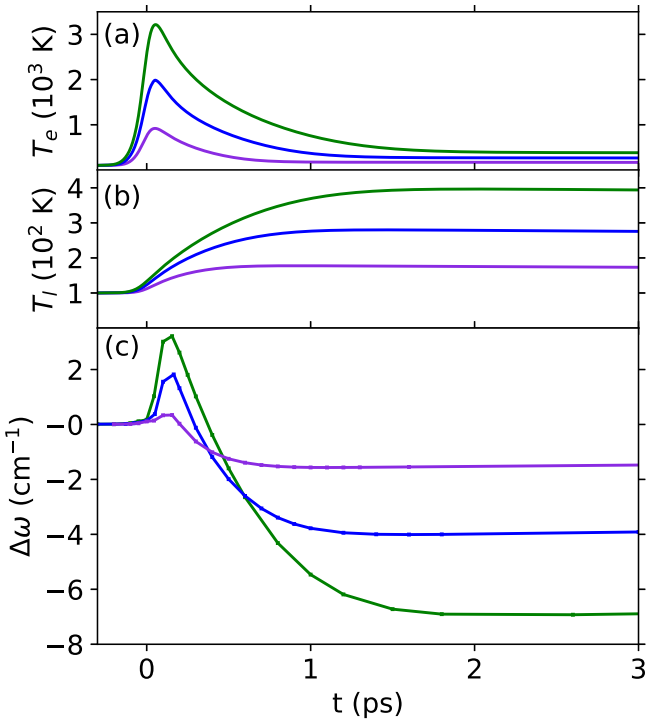

FIG. 3. Transient changes induced in CO/Pd(111) by a 450 nm pump pulse (100 fs duration) with different absorbed fluences: $F = 6$ (purple lines), 19 (blue lines), and 40 J/m^2 (green lines). The pulse maximum is at $t = 0.1$ ps and the system initial temperature is 100 K. (a) Electron temperature $T_e(t)$, (b) lattice temperature $T_l(t)$, and (c) transient frequency shift of the CO IS mode $\Delta\omega(t)$.

initial blueshift that is observed in the initial stage dynamics of Fig. 1(b) is a direct consequence of the electronic structure. This mechanism competes with the strength of the *e*-ph coupling that tends to redshift the frequency as T_e increases. It is only for extreme large electronic temperatures that the latter will dominate the frequency change. Therefore, the next step is to elucidate how the amount of energy that is deposited on the system affects the IS mode dynamics.

We compare in Fig. 3 the results obtained for three different pump laser absorbed fluences: $F = 6$, 19, and 40 J/m^2. Figure 3(c) shows that the behavior of the transient frequency shift $\Delta\omega(t)$ is qualitatively similar for the three absorbed fluences. Both the fast initial blueshift and the subsequent steady redshift increase in magnitude as F increases. In particular, for the lowest fluence of 6 J/m^2, the highest T_e values of about 1000 K [see Fig. 3(a)] are clearly insufficient to induce a sizable blueshift in the frequency. However, we expect it to be experimentally accessible for fluences as low as 19 J/m^2, provided that T_e temporally reaches values of ≈ 2000 K, as shown in Fig. 3(a). Let us finally remark that in experiments the pump pulse creates a nonequilibrium electron distribution during the first tenths of femtoseconds that is not included in our calculations. This could introduce a competing mechanism that eventually may affect the initial transient blueshift. However, considering that the inelastic lifetime of electrons in Pd (around 10 fs [37]) is much smaller than the width of the pump pulse (100 fs) and that thermalization occurs continuously, the nonequilibrated electrons in this system are expected to thermalize very rapidly without masking the predicted blueshift.

In summary, our calculations reveal that the *e*-ph interaction can be screened upon femtosecond laser pulse irradiation provided the electronic density of states of the system changes abruptly around the Fermi level. In particular, we study the ultrafast transient dynamics of the internal stretch mode of CO adsorbed on Pd(111). To do so, we combine density functional theory with many-body perturbation theory and evaluate the phonon self-energy up to second order in the *e*-ph interaction [17]. This allows us to characterize the two main mechanisms that participate in the vibrational relaxation of the internal stretch mode: the first-order interband nonadiabatic coupling and the intraband electron-mediated phonon-phonon coupling. Under current state-of-the-art femtosecond pump-probe experimental conditions, the large transient electronic temperatures that are induced in the femtosecond regime (with $T_e \gg T_l$) give rise to an unconventional blueshift in its frequency. The latter is followed in the picosecond regime by a redshift, larger in magnitude. We show that the initial fast blueshift arises purely from temperature-dependent electronic structure effects, while the subsequent redshift occurs due to the coupling of the internal stretch mode with other phononic modes. The similarity of the results presented here and those of Ref. [16] suggests that an analogous mechanism might be behind the blueshift that was observed for CO molecules coordinated to ruthenium tetraphenylporphyrin on a Cu(110), where large planar molecules might introduce localized high-density states close to the Fermi level in equivalence to the *d* states in the present case. Our results are accessible to current experimental setups and we hope they will stimulate further research on the ultrafast dynamics of polar molecules on complex metallic surfaces with localized states.

The authors acknowledge financial support by the Gobierno Vasco-UPV/EHU Project No. IT1569-22 and the Spanish Ministerio de Ciencia e Innovación (Grant No. PID2019-107396GB-I00/AEI/10.13039/501100011033). R.B. also acknowledges European Union-NextGenerationEU, Ministry of Universities and Recovery, Transformation and Resilience Plan, through a call from Polytechnic University of Catalonia. D.N. additionally acknowledges financial support from the Croatian Science Foundation (Grant No. UIP-2019-04-6869). This research was conducted in the scope of the Transnational Common Laboratory (LTC) QuantumChemPhys - Theoretical Chemistry and Physics at the Quantum Scale. Computational resources were provided by the DIPC computing center.

[1] F. Budde, T. F. Heinz, M. M. T. Loy, J. A. Misewich, F. de Rougemont, and H. Zacharias, Femtosecond Time-Resolved Measurement of Desorption, Phys. Rev. Lett. **66**, 3024 (1991).

[2] J. A. Prybyla, H. W. K. Tom, and G. D. Aumiller, Femtosecond Time-Resolved Surface Reaction: Desorption of CO from Cu(111) in < 325 fsec, Phys. Rev. Lett. **68**, 503 (1992).

[3] M. Lawrenz, K. Stépán, J. Güdde, and U. Höfer, Time-domain investigation of laser-induced diffusion of CO on a vicinal Pt(111) surface, Phys. Rev. B **80**, 075429 (2009).
[4] C. Frischkorn and M. Wolf, Femtochemistry at metal surfaces: Nonadiabatic reaction dynamics, Chem. Rev. **106**, 4207 (2006).
[5] J. Y. Park, S. M. Kim, H. Lee, and I. I. Nedrygailov, Hot-electron-mediated surface chemistry: Toward electronic control of catalytic activity, Acc. Chem. Res. **48**, 2475 (2015).
[6] H. Arnolds and M. Bonn, Ultrafast surface vibrational dynamics, Surf. Sci. Rep. **65**, 45 (2010).
[7] S. Yampolsky, D. A. Fishman, S. Dey, E. Hulkko, M. Banik, E. O. Potma, and V. A. Apkarian, Seeing a single molecule vibrate through time-resolved coherent anti-Stokes Raman scattering, Nat. Photonics **8**, 650 (2014).
[8] T. Omiya and H. Arnolds, Coverage dependent non-adiabaticity of CO on a copper surface, J. Chem. Phys. **141**, 214705 (2014).
[9] M. Bonn, C. Hess, S. Funk, J. H. Miners, B. N. J. Persson, M. Wolf, and G. Ertl, Femtosecond Surface Vibrational Spectroscopy of CO Adsorbed on Ru(001) during Desorption, Phys. Rev. Lett. **84**, 4653 (2000).
[10] I. M. Lane, D. A. King, Z.-P. Liu, and H. Arnolds, Real-Time Observation of Nonadiabatic Surface Dynamics: The First Picosecond in the Dissociation of NO on Iridium, Phys. Rev. Lett. **97**, 186105 (2006).
[11] I. M. Lane, Z.-P. Liu, D. A. King, and H. Arnolds, Ultrafast vibrational dynamics of NO and CO adsorbed on an iridium surface, J. Phys. Chem. C **111**, 14198 (2007).
[12] F. Fournier, W. Zheng, S. Carrez, H. Dubost, and B. Bourguignon, Ultrafast Laser Excitation of CO/Pt(111) Probed by Sum Frequency Generation: Coverage Dependent Desorption Efficiency, Phys. Rev. Lett. **92**, 216102 (2004).
[13] K. Watanabe, K.-i. Inoue, I. F. Nakai, and Y. Matsumoto, Nonadiabatic coupling between C-O stretching and Pt substrate electrons enhanced by frustrated mode excitations, Phys. Rev. B **81**, 241408(R) (2010).
[14] K.-i. Inoue, K. Watanabe, and Y. Matsumoto, Instantaneous vibrational frequencies of diffusing and desorbing adsorbates: CO/Pt(111), J. Chem. Phys. **137**, 024704 (2012).
[15] K.-i. Inoue, K. Watanabe, T. Sugimoto, Y. Matsumoto, and T. Yasuike, Disentangling Multidimensional Nonequilibrium Dynamics of Adsorbates: CO Desorption from Cu(100), Phys. Rev. Lett. **117**, 186101 (2016).
[16] T. Omiya, Y. Kim, R. Raval, and H. Arnolds, Ultrafast vibrational dynamics of CO ligands on RuTPP/Cu(110) under photodesorption conditions, Surfaces **2**, 117 (2019).
[17] D. Novko, J. C. Tremblay, M. Alducin, and J. I. Juaristi, Ultrafast Transient Dynamics of Adsorbates on Surfaces Deciphered: The Case of CO on Cu(100), Phys. Rev. Lett. **122**, 016806 (2019).
[18] A. P. Baddorf and E. W. Plummer, Enhanced Surface Anharmonicity Observed in Vibrations on Cu(110), Phys. Rev. Lett. **66**, 2770 (1991).
[19] G. Bracco, L. Bruschi, L. Pedemonte, and R. Tatarek, Anharmonic effects at the onset of the Ag(110) roughening transition, Surf. Sci. **352–354**, 964 (1996).
[20] D. Novko, M. Alducin, M. Blanco-Rey, and J. I. Juaristi, Effects of electronic relaxation processes on vibrational linewidths of adsorbates on surfaces: The case of CO/Cu(100), Phys. Rev. B **94**, 224306 (2016).
[21] D. Novko, M. Alducin, and J. I. Juaristi, Electron-Mediated Phonon-Phonon Coupling Drives the Vibrational Relaxation of CO on Cu(100), Phys. Rev. Lett. **120**, 156804 (2018).
[22] H. Hayashi, K. Shimada, J. Jiang, H. Iwasawa, Y. Aiura, T. Oguchi, H. Namatame, and M. Taniguchi, High-resolution angle-resolved photoemission study of electronic structure and electron self-energy in palladium, Phys. Rev. B **87**, 035140 (2013).
[23] V. Schendel, C. Barreteau, M. Brandbyge, B. Borca, I. Pentegov, U. Schlickum, M. Ternes, P. Wahl, and K. Kern, Strong paramagnon scattering in single atom Pd contacts, Phys. Rev. B **96**, 035155 (2017).
[24] F. Giustino, Electron-phonon interactions from first principles, Rev. Mod. Phys. **89**, 015003 (2017).
[25] R. Bauer, A. Schmid, P. Pavone, and D. Strauch, Electron-phonon coupling in the metallic elements Al, Au, Na, and Nb: A first-principles study, Phys. Rev. B **57**, 11276 (1998).
[26] S. I. Anisimov, B. L. Kapeliovich, and T. L. Perel'man, Electron emission from metal surfaces exposed to ultrashort laser pulses, Sov. Phys. JETP **39**, 375 (1974).
[27] M. Rose, T. Mitsui, J. Dunphy, A. Borg, D. Ogletree, M. Salmeron, and P. Sautet, Ordered structures of CO on Pd(111) studied by STM, Surf. Sci. **512**, 48 (2002).
[28] J. Wellendorff, K. T. Lundgaard, A. Møgelhøj, V. Petzold, D. D. Landis, J. K. Nørskov, T. Bligaard, and K. W. Jacobsen, Density functionals for surface science: Exchange-correlation model development with Bayesian error estimation, Phys. Rev. B **85**, 235149 (2012).
[29] P. Giannozzi, S. Baroni, N. Bonini, M. Calandra, R. Car, C. Cavazzoni, D. Ceresoli, G. L. Chiarotti, M. Cococcioni, I. Dabo, A. Dal Corso, S. De Gironcoli, S. Fabris, G. Fratesi, R. Gebauer, U. Gerstmann, C. Gougoussis, A. Kokalj, M. Lazzeri, L. Martin-Samos *et al.*, QUANTUM ESPRESSO: A modular and open-source software project for quantum simulations of materials, J. Phys.: Condens. Matter **21**, 395502 (2009).
[30] P. Giannozzi, O. Andreussi, T. Brumme, O. Bunau, M. Buongiorno Nardelli, M. Calandra, R. Car, C. Cavazzoni, D. Ceresoli, M. Cococcioni, N. Colonna, I. Carnimeo, A. Dal Corso, S. De Gironcoli, P. Delugas, R. A. Distasio, A. Ferretti, A. Floris, G. Fratesi, G. Fugallo *et al.*, Advanced capabilities for materials modelling with Quantum ESPRESSO, J. Phys.: Condens. Matter **29**, 465901 (2017).
[31] J. Noffsinger, F. Giustino, B. D. Malone, C.-H. Park, S. G. Louie, and M. L. Cohen, Epw: A program for calculating the electron–phonon coupling using maximally localized Wannier functions, Comput. Phys. Commun. **181**, 2140 (2010).
[32] S. Poncé, E. Margine, C. Verdi, and F. Giustino, Epw: Electron–phonon coupling, transport and superconducting properties using maximally localized Wannier functions, Comput. Phys. Commun. **209**, 116 (2016).
[33] See Supplemental Material at http://link.aps.org/supplemental/10.1103/PhysRevB.107.L121404 for all the computational details that are needed to reproduce the results presented in this Letter. It also includes a discussion about the importance of the chemical potential shift, which includes Refs. [38–56].
[34] B. N. J. Persson and R. Ryberg, Vibrational Phase Relaxation at Surfaces: CO on Ni(111), Phys. Rev. Lett. **54**, 2119 (1985).
[35] J. C. Cook, S. K. Clowes, and E. M. McCash, Reflection absorption ir studies of vibrational energy transfer processes and

adsorption energetics, J. Chem. Soc. Faraday Trans. **93**, 2315 (1997).

[36] J. Sky Zhou, R. Bianco, L. Monacelli, I. Errea, F. Mauri, and M. Calandra, Theory of the thickness dependence of the charge density wave transition in 1T-$TiTe_2$, 2D Mater. **7**, 045032 (2020).

[37] V. P. Zhukov, F. Aryasetiawan, E. V. Chulkov, and P. M. Echenique, Lifetimes of quasiparticle excitations in 4*d* transition metals: Scattering theory and LMTO-RPA-GW approaches, Phys. Rev. B **65**, 115116 (2002).

[38] A. Dal Corso, Pseudopotentials periodic table: From H to Pu, Comput. Mater. Sci. **95**, 337 (2014).

[39] H. J. Monkhorst and J. D. Pack, Special points for Brillouin-zone integrations, Phys. Rev. B **13**, 5188 (1976).

[40] V. Vitale, G. Pizzi, A. Marrazzo, J. R. Yates, N. Marzari, and A. A. Mostofi, Automated high-throughput Wannierisation, npj Comput. Mater. **6**, 66 (2020).

[41] A. A. Mostofi, J. R. Yates, Y.-S. Lee, I. Souza, D. Vanderbilt, and N. Marzari, Wannier90: A tool for obtaining maximally-localised Wannier functions, Comput. Phys. Commun. **178**, 685 (2008).

[42] N. Marzari, A. A. Mostofi, J. R. Yates, I. Souza, and D. Vanderbilt, Maximally localized Wannier functions: Theory and applications, Rev. Mod. Phys. **84**, 1419 (2012).

[43] A. A. Mostofi, J. R. Yates, G. Pizzi, Y.-S. Lee, I. Souza, D. Vanderbilt, and N. Marzari, An updated version of Wannier90: A tool for obtaining maximally-localised Wannier functions, Comput. Phys. Commun. **185**, 2309 (2014).

[44] G. Pizzi, V. Vitale, R. Arita, S. Blügel, F. Freimuth, G. Géranton, M. Gibertini, D. Gresch, C. Johnson, T. Koretsune, J. Ibañez-Azpiroz, H. Lee, J.-M. Lihm, D. Marchand, A. Marrazzo, Y. Mokrousov, J. I. Mustafa, Y. Nohara, Y. Nomura, L. Paulatto *et al.*, Wannier90 as a community code: new features and applications, J. Phys.: Condens. Matter **32**, 165902 (2020).

[45] W. M. Haynes, D. R. Lide, and T. J. Bruno, *CRC Handbook of Chemistry and Physics* (CRC press, New York, 2016).

[46] K. Nakamoto, *Handbook of Vibrational Spectroscopy* (Wiley, Hoboken, NJ, 2006).

[47] A. Bradshaw and F. Hoffmann, The chemisorption of carbon monoxide on palladium single crystal surfaces: Ir spectroscopic evidence for localised site adsorption, Surf. Sci. **72**, 513 (1978).

[48] T Gießel, O. Schaff, C. Hirschmugl, V. Fernandez, K.-M. Schindler, A. Theobald, S. Bao, R. Lindsay, W. Berndt, A. Bradshaw, C. Baddeley, A. Lee, R. Lambert, and D. Woodruff, A photoelectron diffraction study of ordered structures in the chemisorption system Pd(111)-CO, Surf. Sci. **406**, 90 (1998).

[49] N. W. Ashcroft and N. D. Mermin, *Solid State Physics* (Saunders College Publishing, Philadelphia, 1988).

[50] C. Kittel, *Introduction to Solid State Physics*, 6th ed. (Wiley, New York, 1986).

[51] P. Johnson and R. Christy, Optical constants of transition metals: Ti, V, Cr, Mn, Fe, Co, Ni, and Pd, Phys. Rev. B **9**, 5056 (1974).

[52] P. Szymanski, A. Harris, and N. Camillone, Temperature-dependent electron-mediated coupling in subpicosecond photoinduced desorption, Surf. Sci. **601**, 3335 (2007).

[53] S.-Y. Hong, P. Xu, N. R. Camillone, M. G. White, and N. Camillone, Adlayer structure dependent ultrafast desorption dynamics in carbon monoxide adsorbed on Pd (111), J. Chem. Phys. **145**, 014704 (2016).

[54] Y. Li and P. Ji, *Ab initio* calculation of electron temperature dependent electron heat capacity and electron-phonon coupling factor of noble metals, Comput. Mater. Sci. **202**, 110959 (2022).

[55] J. M. Luttinger, Fermi surface and some simple equilibrium properties of a system of interacting fermions, Phys. Rev. **119**, 1153 (1960).

[56] F. Andreatta, H. Rostami, A. G. Čabo, M. Bianchi, C. E. Sanders, D. Biswas, C. Cacho, A. J. H. Jones, R. T. Chapman, E. Springate, P. D. C. King, J. A. Miwa, A. Balatsky, S. Ulstrup, and P. Hofmann, Transient hot electron dynamics in single-layer TaS_2, Phys. Rev. B **99**, 165421 (2019).